

Electron localization in metallic quantum wells: Pb versus In on Si(111)

J. H. Dil, J. W. Kim,* Th. Kampen, and K. Horn

Department of Molecular Physics, Fritz-Haber-Institut der Max-Planck-Gesellschaft, Faradayweg 4-6, D-14195 Berlin, Germany

A. R. H. F. Ettema

Department of Nanoscience, Delft University of Technology, Lorentzweg 1, 2628CJ Delft, The Netherlands

(Received 3 April 2006; published 27 April 2006)

Two-dimensional quantum well states in ultrathin metal films generally exhibit a dispersion relation of s - p -derived states that can be described through an effective mass of the corresponding bulk band. By contrast, the effective masses in Pb quantum well states on Si(111), measured through angle-resolved photoemission, are up to an order of magnitude larger than those from the bulk states or predicted by slab calculations, while similar anomalies are not observed in the related In/Si(111) system. We interpret these data in terms of an enhanced electron localization, and use them to interpret recent scanning tunneling microscopy results.

DOI: 10.1103/PhysRevB.73.161308

PACS number(s): 73.21.Fg, 68.55.Jk, 79.60.Dp

The physical properties of ultrathin epitaxial metallic films exhibit marked differences compared to those of the bulk, through the effect of electron confinement in the film, and the influence of film-substrate and film-vacuum interfaces. Electron confinement leads to the formation of discrete quantum well states (QWS),¹ which may play a decisive role in many film properties, such as growth morphology,² “magic” or “critical” thicknesses,³ oscillations in the magnitude of the superconducting transition temperature,⁴ and oscillations in the direction and magnitude of the Hall effect.^{5,6} Moreover, the study of confinement in metal films has led to important observations of fundamental properties of metals, such as a detailed study of electron-phonon coupling.⁷ In extended metal films, electron motion is only confined in the (z) direction normal to the film. Hence, quantum well states are expected to exhibit a dispersion relation $E(k_{\parallel x}, k_{\parallel y})$ for the component of electron wave vector k_{\parallel} along the x and y directions parallel to the film, that is similar to the bulk band from which they are derived. This is in fact found in studies of quantum well states in s - p metals such as Ag,⁸ Al,⁹ and Mg.¹⁰ Effective masses m^* are used to describe the dispersion with the parallel component of the wave vector k_{\parallel} in these s - p -derived bands, $E = \hbar^2 k_{\parallel}^2 / 2m^*$. As determined experimentally from angle-resolved photoemission studies, they generally agree well with those from theoretical calculations based on free-standing films. This indicates that the influence of interface structure and confinement on this aspect of electron dynamics is negligible. However, there are cases in which a marked change in effective mass has been suggested.¹¹ We show that in the Pb/Si(111) system, a widely used model for metallic quantum wells,¹² the effective mass m^* of the Pb- $6p_z$ band is increased dramatically in Pb quantum wells, while no deviation from the normal behavior in other metallic quantum well systems is found in In/Si(111). Due to the fact that indium is, similar to lead, nonreactive with silicon, has almost exactly the same lattice constant (albeit with a different structure), and is also an s - p metal with only one valence electron less, In/Si(111) is closely related to Pb/Si(111). We conclude that the observed effects are due to an enhanced electron localization, and dis-

cuss its occurrence in this particular system. Recent scanning tunneling microscopy (STM) results are interpreted in terms of our data.

The experiments were performed in a μ -metal ultrahigh vacuum chamber with a base pressure better than 3×10^{-10} mbar. An n -doped Si(111) sample was cleaned by flashing to 1200 °C. Surface cleanliness was confirmed by the presence of surface states and a 7×7 reconstruction. The Si(111):Pb $\sqrt{3} \times \sqrt{3} R30^\circ$ surface reconstruction [henceforth referred to as Si(111) $\sqrt{3}$] was obtained by low-temperature deposition of 2.5 monolayers (ML) of Pb on the clean Si(111), followed by an anneal to around 350 °C. After cooling down again to 110 K, the $\sqrt{3} \times \sqrt{3} R30^\circ$ surface reconstruction was confirmed with low-energy electron diffraction (LEED). Pb was evaporated on top of this surface from a homemade Knudsen cell at a deposition rate of 0.18 ML per minute. Similar results were found for Pb layers deposited on the clean Si(111) 7×7 surface. Indium layers were deposited in a similar manner onto clean Si(111) 7×7 , at a sample temperature of 60 K. The measurements were performed at the TGM-4 and 10 m NIM beamlines at BESSY in Berlin. Data were recorded with a Phoibos 100 analyzer equipped with a two-dimensional (2D) CCD detector (Specs GmbH, Berlin). We compare our experimental data with local-density approximation (LDA) band structure calculations, which were performed with the localized spherical wave method as described by v. Leuken *et al.*,¹³ is adapted from the augmented spherical wave (ASW) method.¹⁴ The Pb quantum well is modeled by a slab of 10 monolayers Pb separated by 10 monolayers of empty spheres.

Angle-resolved photoemission is ideally suited to determine electronic band dispersions in a wide variety of systems,¹⁵ and in electron energy analyzers, which permit a display of $E(k)$ in an imaging mode, patterns due to emission from band states can be directly observed. Consider the photoemission intensity plots, given as a function of electron wave vector k_{\parallel} and energy below the Fermi level E_F , for the Pb/Si(111) and In/Si(111) systems in Fig. 1. Both sets of data were recorded for the same thickness. They exhibit the quantum well states derived from the Pb- $6p_z$ and In- $5p_z$

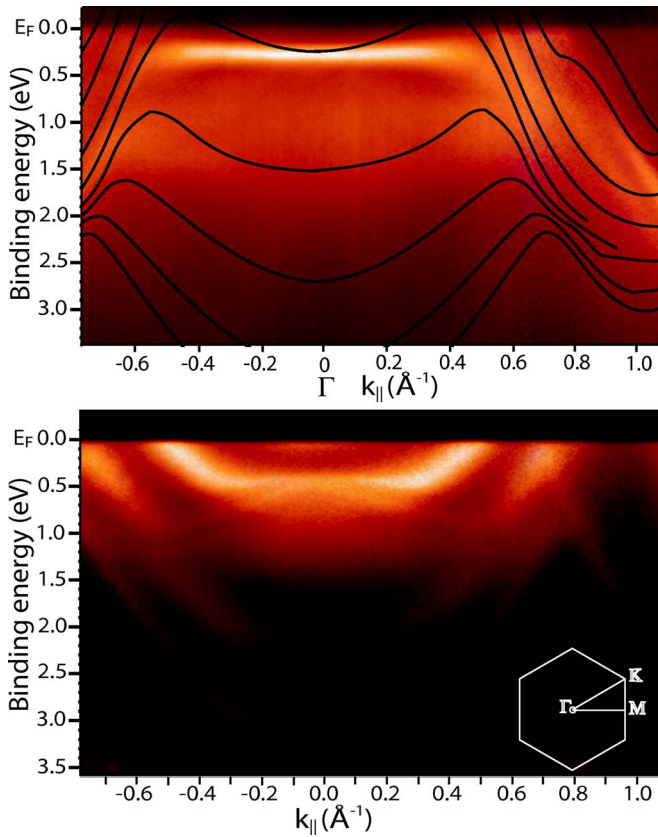


FIG. 1. (Color online) (Top) In-plane dispersion of Pb quantum well states for a 10 ML thick Pb film on Si(111) $\sqrt{3}$ along the $\bar{\Gamma}$ - \bar{M} direction in the 2D Brillouin zone. The black lines show the calculated band dispersion (see text). (Bottom) In-plane dispersion of In quantum well states for a 10 ML film of In/Si(111). (Inset) Surface Brillouin zone for the Pb layers.

bands at $k_{||}=0$. It is obvious that their dispersion with $k_{||}$ is markedly different. First, a strong interaction with the top-most silicon valence band occurs in the indium data, and to a lesser extent in the Pb data (see also Fig. 2). This interaction has also been observed in other systems, for example, Ag on Ge.¹⁶ In determining the effective masses, we take this effect into account, as described below, i.e., we fit the free-electron-

like parabola only to the region where the interaction with the substrate bands is absent. For the indium data in Fig. 1, this restricts the analysis to the region $0.35 < k_{||} < 0.6 \text{ \AA}^{-1}$. However, it is obvious, even from this small range, that the curvature of the dispersion is very different from that of the QWS in Pb. Applying this detailed analysis of effective masses, based on a fitting of lines for different $k_{||}$, results in a factor 7 difference, i.e., $m^* = 1.2$ for In/Si(111) and $m^* = 8$ for Pb/Si(111) $\sqrt{3}$.

Inserted in the Pb figure is a slab calculation of electron states in thin Pb films based on the density functional theory (DFT) as described above. The features dispersing downward toward the edge of the Brillouin zone, crossing the Fermi level at approximately 0.6 \AA^{-1} , are related to the $6p_x$ and $6p_y$ states; this behavior is reproduced in the experimental data. However, there is a strong discrepancy between calculations and measurement in the dispersion of the quantum well states near the center of the Brillouin zone. The calculations show a free-electron-like behavior with an effective mass varying from $0.6 m_e$ at 4 eV below E_F to $2 m_e$ at 6 eV above E_F (not included). Contrary to the LDA calculations the measured QWS band hardly disperses at all.

The effective masses of quantum well states show a decreasing trend with coverage. This is to be expected, since in the limit of thick films, approaching the bulk regime, m^* should reach the corresponding value for the bulk band. Figure 2 shows the in-plane dispersion close to the Brillouin zone center for films of 17 and 22 ML thickness on Si(111) $\sqrt{3}$. Even for films of 22 ML, the effective mass is $5.2 m_e$ for the highest occupied quantum well state. Effective mass values were obtained by taking slices through the image every 0.023 \AA^{-1} , which results in a set of electron distribution curves similar to those measured with a single channel angle-resolved electron energy analyzer. These spectra were then fitted to obtain peak positions for the QWS as a function of in-plane momentum. By accurately analyzing the features in the images, spectra, and fits, the QWS can be distinguished from any substrate features that are in the same region, in a manner comparable to studies by Aballe *et al.*¹⁷

Figure 2(c) shows the result of a fit performed in this manner for the 10 ML film, where the binding energy range is magnified compared to the other images. The upward pa-

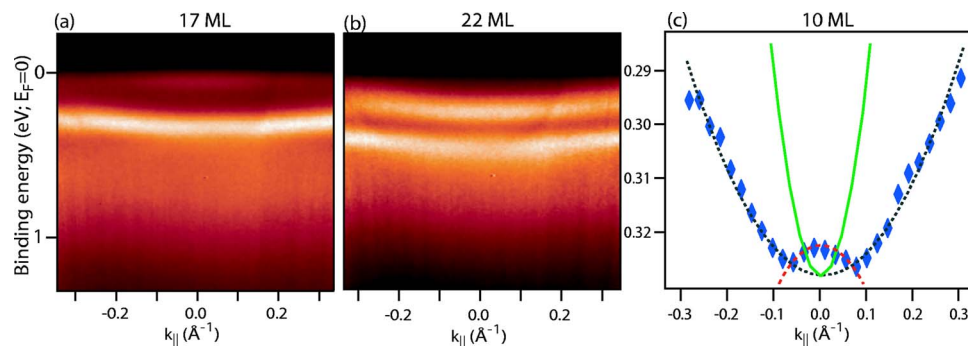


FIG. 2. (Color online) In-plane dispersion for (a) 17 and (b) 22 ML of Pb on Si(111) $\sqrt{3}$. (c) Data points for the position of the QWS in a 10 ML Pb film on Si(111) $\sqrt{3}$ (from the data in Fig. 1), with a parabolic fit to extract the effective mass (black dotted line) and to account for the downward dispersing Si feature (red dashed line). The solid green parabola represents the dispersion expected from calculations. Note the enlarged energy scale in (c).

parabola of the QWS can be clearly distinguished from the downward parabola from the topmost valence band edge of the Si(111) substrate (red dashed line). The black dotted line indicates the fit performed to extract the effective mass for the Pb quantum well state. For clarity, the dispersion expected from DFT calculations is represented by the green solid line.

The development of quantum well features with coverage (Fig. 2) demonstrates that the films grow in a smooth, layer-by-layer manner, since no features are observed from a mixture of thicknesses. This is also confirmed by the sharpness of the observed LEED spots. Quantum well states are mainly observed above the valence band edge of the silicon substrate, except for the small overlap in Fig. 2(c), showing that effective confinement occurs mainly in the Si fundamental band gap. This corresponds very well to other observations for this system.¹⁸

The magnitude of the effective mass parameter, which serves to describe the bands above, is related to the localization of states from which they are derived. However, in this interpretation based on effective masses from dispersing quantum well bands, other factors that may influence their dispersion also need to be considered. One of these is the phase shift of the electron waves at the interface. In the so-called phase accumulation model,¹⁹ the existence of quantum well states is governed by the Bohr-Sommerfeld quantization rule

$$2k_{\perp}Na + \phi_b + \phi_c = 2\pi n, \quad (1)$$

where N is the number of layers, a is the layer thickness, n is an integer, and ϕ_b , ϕ_c are the phase shifts at the vacuum and substrate sides, respectively. The value for the phase shifts is generally a function of energy and k_{\perp} , and a change of the accumulated ϕ 's by an amount on the order of π might significantly alter the observed binding energies, and might possibly be able to mimic a larger effective mass. Upton *et al.*²⁰ have explained the large effective masses in Pb/Si quantum well states along this line of argument, on the basis of the interaction between the quantum well states and the silicon bulk bands. This interaction ("hybridization") causes the bands to repel, leading to an *apparent* increase of m^* , an explanation that may be rephrased by postulating a k_{\parallel} -dependent phase shift of the electrons in the quantum well at the Pb-Si interface. Wu *et al.*²¹ have suggested that the influence of the bands in the substrate on the phase shift at the interface can be substantial for metallic substrates. The band dispersion in their substrate (cobalt) is, however, opposite to that in Si(111). Moreover, it is comparable to that of Cu, such that for Pb on Cu a similar effect as described should be expected, whereas for Pb on silicon the effect should be the opposite. In contrast, for Pb layers on Cu(111) no increase in the effective mass has been observed in coverages above 3 ML.²² The fact that we observe large effective masses even in layers of more than 22 ML thickness, where according to Eq. (1) the influence of the phase shift at the interface is necessarily small, also renders this explanation unlikely. In Fig. 3, we show the dependence of the effective mass in lead and indium films on Si(111) as a function of coverage and binding energy. While the effective

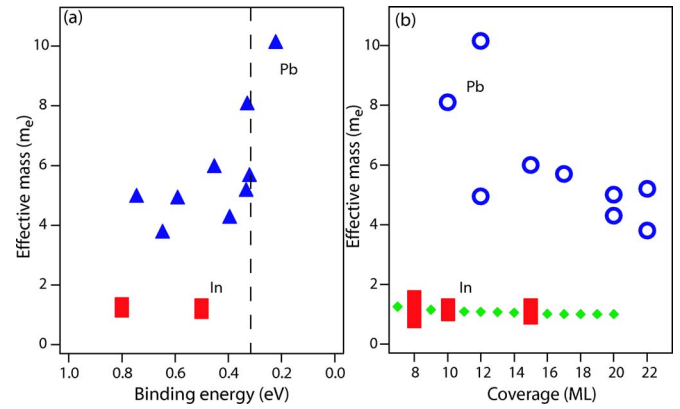


FIG. 3. (Color online) Effective mass as a function of binding energy (a) and coverage (b). The blue upward triangles and circles are for the Pb QWS, the red squares are for the In QWS. For clarity, the theoretically calculated effective mass has been inserted in (b) as green diamonds. The dashed line in (a) represents the Si valence band maximum.

mass exhibits an increase in Pb films for QW states near E_F , it remains large even for states well below the onset of the Si substrate bands. The trend with thickness shows that even for 22 ML films there is a large discrepancy between the calculated and experimental data.

The interpretation of a k_{\parallel} -dependent phase shift to account for an enhancement of m^* is thus at variance with our above results and other data. The interaction between the silicon bulk bands and the QWS bands is seen to be clearly restricted to a small region of k space and does not affect our determination of m^* . Moreover, it does not explain the absence of an effective mass increase for the QWS in indium layers on the same substrate (see Fig. 1), since the shape of the substrate bands is the key ingredient in this argument (for a plot of trends in m^* with thickness and binding energy for these two systems, see Fig. 3). For Ag, Al, and Mg films on Si(111), where s - p -type bands cover the range from well below the band edge up to the Fermi level, across the fundamental band-gap edge, again no effect is seen, and effective masses agree with bulk values and/or slab calculations.^{9,10,23} There is no dependence of the effective mass on the structural details at the interface, since it occurs for Pb films on the bare Si(111) 7×7 as well as on the reconstructed $\sqrt{3}$ surface.

Having thus excluded an influence of the interface and substrate bands that might lead to the unusual band dispersion, and considering the large differences between the indium and Pb data, we are led to consider that the electron states in the Pb quantum wells exhibit a higher degree of in-plane localization. X-ray diffraction (XRD) studies of the Pb/Si(111) system have revealed a bilayer oscillation in the interlayer spacing,²⁴ persisting also for higher coverages, that are not present in bulk Pb data. This indicates that the layer is not fully relaxed in the direction perpendicular to the substrate. In Fig. 1, the $6p_{x,y}$ states are seen to behave as expected from theory, the localization is only present in the $6p_z$ states. Therefore, we suggest that there occurs a structural alteration, which minimizes the overlap of the $6p_z$ states in the direction parallel to the surface.

A thickness- and energy-dependent change in quantum well state dispersion caused by enhanced electron localization is supported by other experimental observations. First, the Hall effect in thin Pb films on Si(111) shows an oscillatory reversal of sign as a function of thickness,⁵ indicating a size quantization effect on the specific resistivity. This observation cannot be fully explained on the basis of electron confinement based either on free-electron-like states, or on details of the Pb band structure in the (111) direction.⁶ A consideration of the large in-plane effective masses found here might be useful for an interpretation of the Hall effect observations. Second, Altfeder and co-workers have observed, in scanning tunneling microscopy experiments, that the Si(111) 7×7 reconstruction can be imaged through Pb layers of more than 100 Å thickness,²⁵ suggesting that the lateral spread of electrons injected into the layer is extremely small; a similar effect in indium layers is restricted to very small thicknesses. As shown in Fig. 3, at a coverage above 8 ML the effective masses in indium QWS are similar to those of bulk bands. Altfeder and co-workers have interpreted this result in terms of a large anisotropy of the effective masses associated with in-plane and transverse electron motion. The observation of atomic scale features in tunneling experiments of electrons transmitted through a Pb layer of considerable thickness on Si(111) shows that the “defocusing” of the tunneling electrons in an energy region close to the Fermi level is extremely small, demonstrating the lateral

localization of such states. An in-depth interpretation of our unusual results has to await theoretical treatment, which includes the Pb/Si(111) interface. However, band structure calculations for this system have to take into account the large lattice mismatch, a serious complication, and (except for one attempt in which the Si lattice constant was artificially reduced by 9%,¹⁸ actually resulting in a metallic substrate) are not yet available.

In conclusion, our angle-resolved photoemission results show that the lateral effective masses in Pb quantum well states on Si(111) are up to an order of magnitude larger than those from the bulk states or predicted by slab calculations. From a comparison with related metallic quantum well systems on Si(111), and in agreement with recent suggestions from scanning tunneling microscopy studies, we interpret these results in terms of strongly enhanced lateral electron localization.

This work was supported as part of the European Science Foundation EUROCORES programme SONS under programme MOL-VIC through funds from the Deutsche Forschungsgemeinschaft, and the EC Sixth Framework programme. J.H.D. acknowledges support by the International Max-Planck Research School “Complex Surfaces in Material Sciences.” J.W.K. acknowledges support by the Alexander von Humboldt Foundation. We gratefully acknowledge support by the BESSY staff.

*Present address: Korea Research Institute of Standards and Science, P.O. Box 102, Daejeon 305–600, Korea.

¹T.-C. Chiang, *Surf. Sci. Rep.* **39**, 181 (2000).

²K. Budde, E. Abram, V. Yeh, and M. C. Tringides, *Phys. Rev. B* **61**, R10602 (2000).

³Z. Zhang, Q. Niu, and C. K. Shih, *Phys. Rev. Lett.* **80**, 5381 (1998).

⁴B. G. Orr, H. M. Jaeger, and A. M. Goldman, *Phys. Rev. Lett.* **53**, 2046 (1984).

⁵M. Jalochowski, M. Hoffmann, and E. Bauer, *Phys. Rev. Lett.* **76**, 4227 (1996).

⁶I. Vilfan, M. Henzler, O. Pfennigstorf, and H. Pfñür, *Phys. Rev. B* **66**, 241306 (2002).

⁷J. J. Paggel, D.-A. Luh, T. Miller, and T.-C. Chiang, *Phys. Rev. Lett.* **92**, 186803 (2004).

⁸M. A. Mueller, T. Miller, and T.-C. Chiang, *Phys. Rev. B* **41**, 5214 (1990).

⁹L. Aballe, C. Rogero, S. Gokhale, S. Kulkarni, and K. Horn, *Surf. Sci.* **482–485**, 488 (2001).

¹⁰L. Aballe, C. Rogero, and K. Horn, *Phys. Rev. B* **65**, 125319 (2002).

¹¹I. B. Altfeder, X. Liang, T. Yamada, D. M. Chen, and V. Narayanamurti, *Phys. Rev. Lett.* **92**, 226404 (2004).

¹²I. B. Altfeder, J. A. Golovchenko, and V. Narayanamurti, *Phys. Rev. Lett.* **87**, 056801 (2001).

¹³H. v. Leuken, A. Lodder, M. T. Czyzyk, F. Springelkamp, and R. A. de Groot, *Phys. Rev. B* **41**, 5613 (1990).

¹⁴A. R. Williams, J. Kübler, and C. D. Gelatt, Jr., *Phys. Rev. B* **19**, 6094 (1979).

¹⁵S. D. Kevan, *Angle Resolved Photoemission* (Elsevier Science, Amsterdam 1992).

¹⁶S.-J. Tang, T. Miller, and T.-C. Chiang, *Phys. Rev. Lett.* **96**, 036802 (2006).

¹⁷L. Aballe, C. Rogero, P. Kratzer, S. Gokhale, and K. Horn, *Phys. Rev. Lett.* **87**, 156801 (2001).

¹⁸M. H. Upton, C. M. Wei, M. Y. Chou, T. Miller, and T.-C. Chiang, *Phys. Rev. Lett.* **93**, 026802 (2004).

¹⁹P. Echenique and J. B. Pendry, *J. Phys. C* **11**, 2065 (1978); N. V. Smith, *Phys. Rev. B* **32**, 3549 (1985).

²⁰M. H. Upton, T. Miller, and T. C. Chiang, *Phys. Rev. B* **71**, 033403 (2005).

²¹Y. Z. Wu, C. Y. Won, E. Rotenberg, H. W. Zhao, F. Toyoma, N. V. Smith, and Z. Q. Qin, *Phys. Rev. B* **66**, 245418 (2002).

²²J. H. Dil, J. W. Kim, S. Gokhale, M. Tallarida, and K. Horn, *Phys. Rev. B* **70**, 045405 (2004).

²³G. Neuhold, Ph.D. thesis, Freie Universität Berlin, 1997.

²⁴P. Czoschke, Hawoong Hong, L. Basile, and T.-C. Chiang, *Phys. Rev. Lett.* **91**, 226801 (2003).

²⁵I. B. Altfeder, D. M. Chen, and K. A. Matveev, *Phys. Rev. Lett.* **80**, 4895 (1998).